Quantum Dot-DNA Origami Binding: A Single Particle, 3D, Real-Time Tracking Study

Kan Du,[a,b, ‡] **Seung Hyeon Ko,**[a,b, ‡] **Gregg M. Gallatin,**[a] **Heayoung Yoon,**[a,b] **J. Alexander Liddle*,**[a] **and Andrew J. Berglund*,**[a]

The binding process of quantum dots and DNA origami was monitored using a 3D, real-time, single-particle tracking system. Single-molecule binding events were directly observed and precise measurements of the diffusion coefficient and second-order photon correlation function, $g^2(\tau)$, were combined to distinguish free quantum dots from different conjugates of nQdot-origami.

DNA origami[1] is being actively investigated as a template to organize diverse nanoscale objects with molecular precision. Small assemblages of inorganic nanoparticles arranged in this way are of great interest because of potential applications in sensors, drug delivery systems and optical devices.[2-8] To assemble such nanostructures with high yields, the various aspects of the dynamic particle-origami binding process must be undertsood.[8] We have focused on the development of experimental methods to measure DNA origami binding reaction kinetics.[8]

Here we present results obtained by *in situ* monitoring of quantum dot (Qdot) binding to individual DNA origami in their native state, in solution using a three-dimensional (3D), real-time, single-particle tracking system.[9] Specifically, the measurements rely on the single-molecule tracking system's ability to identify unambiguously a variety of fluorescent species by simultaneous analysis of the diffusion coefficient (D) and the second-order photon correlation function $g^2(\tau)$,[10,11] of each tracked object. We note that gel electrophoresis cannot resolve the different species, since the various origami-Qdot conjugates exhibit minimal differences in charge/mobility (see Fig. S1). A major advantage of this approach is its ability to track and identify intermediate fluorescent species formed during the reaction without the need for any purification or isolation. This enables the observation of processes in a way that might not otherwise be possible.

In this work we use rectangular DNA origami (70 nm x 100 nm)[1] engineered to have 1, 2 or 3 binding sites. Each binding site consists of a set of three closely-spaced (≈ 5 nm) biotinylated staple strands to capture a streptavidin-functionalized Qdot. The tracking system enables us to follow individual Qdots and a variety of conjugates of nQdot-DNA origami (n is the number of Qdots, 1, 2 or 3, bound to an origami), as illustrated in Fig. 1(a). Individual species were tracked for approximately 30 s. 3D positional data is analyzed to yield the diffusion coefficient using the mean square displacement as a function of time. The fluorescence signal used for tracking is divided by a 50:50 beam

splitter and the two resulting photon streams are detected by single photon-detectors. The photon arrival times are used to determine $g^2(\tau)$.
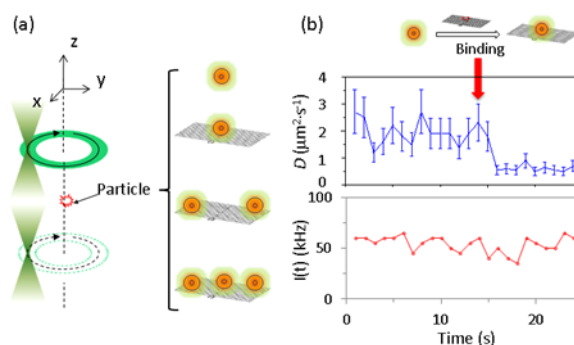
Fig. 1 (a) Schematic representation of the single-particle tracking process of nQdot-DNA origami (n is the number of Qdots, 1, 2 or 3, bound to an origami). A piezo stage, under feedback control via the fluorescence signal, is used to lock a fluorescent object in the 3D laser-scanning pattern, which consists of two horizontal circles vertically displaced from one another.[9] (b) Representative measurement of diffusion coefficient and fluorescent intensity for a Qdot binding to a DNA origami. Error bars represent one standard deviation in the estimate of the diffusion coefficient, D.[12] When a binding event occurs, the diffusion coefficient decreases abruptly while the fluorescent intensity remains constant.

Two types of event are observed while tracking single species: abrupt reductions in D at constant fluorescent intensity (Fig. 1(b)) indicate that a binding event has occurred, changing the effective hydrodynamic radius of the particle, while changes in average fluorescent intensity with or without a change in D indicate a switching event (Supplementary Information, Fig. S2), in which one tracked emitter is replaced by another.

As a proof of principle, we first investigated the *in situ* binding of single Qdots to DNA origami engineered to have one binding site, producing a 1:1 conjugate, 1Qdot-origami. A DNA origami solution was mixed with streptavidin-coated CdSe/ZnS core/shell Qdots at a stoichiometry of 100 to 1 (1.6 nmol·L^{-1} : 16 pmol·L^{-1}). The excess of the DNA ensures that essentially all the Qdots will bind during the reaction. DNA origami and Qdots were in buffer solutions containing glycerol. After stirring to ensure complete mixing, ≈ 20 μL of solution were transferred to the sample cell for observation. Tracking data were obtained for 18 h and the number of free Qdots and 1Qdot-origami observed were binned in 30 minute intervals. Figure 2 shows data from a typical

experiment. We assume that the number of any given species observed is proportional to the concentration of that species. As can be seen, the number of free Qdots falls and the number of bound Qdots rises over time as the Qdots react with the origami. Note that the initial number of free Qdots observed is less than the final number of bound Qdots. This is a result both of the delay that occurs between mixing of the reagents and the start of observations, and also the fact that the slow moving bound Qdots are easier to track, resulting in a counting bias.
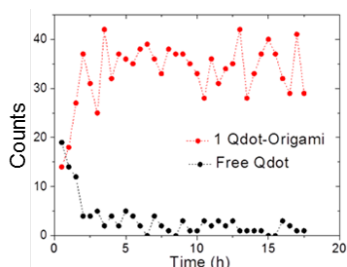
Fig. 2 Binding reaction of Qdots to DNA origami containing a single binding site. The counts (number observed in 30 min increments) of free Qdot decreases as the reaction progresses, while the counts of Qdot-Origami increases. Free and bound Qdots are easily identified by their different diffusion coefficients.
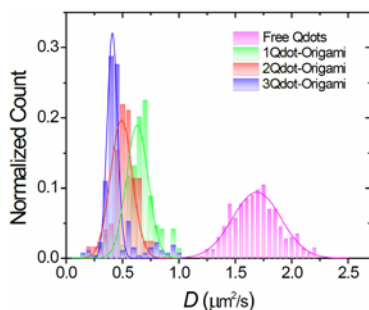
Fig. 3 Normalized measurements of D (bars) and corresponding Gaussian fits (lines) of free Qdots and various n Qdot-DNA origami ($n = 1, 2,$ and 3) calibration samples. These plots enable us to directly identify the different bound species by comparing diffusion coefficient values. The diffusion coefficient data are binned in increments of 0.05 μm^{2}s^{-1}. The standard deviation in each diffusion coefficient measurements is $0.3D$.[12]

For a more complex case, such as the reaction of Qdots with origami containing three binding sites, various nQdot-origami are generated as the reaction proceeds. Identifying the constituent species as a function of time is more challenging, since the changes in diffusion coefficient between, for example, 2Qdot-origami and 3Qdot-origami, are small. To explore this in more detail, we first performed measurements with separately prepared calibration samples to obtain D and $g^2(\tau)$. Calibration samples were engineered to bind a specific number (n) of Qdots to make nQdot-origami conjugates, which were separated from excess DNA and free Qdots by performing agarose gel electrophoresis. Even though the agarose gels and scanning electron microscopy (SEM) imaging analysis (Fig. S1) indicated that each purified conjugate consisted of more than one nQdot-origami species (Fig. S3), the measured D values for the individual samples (Fig. 3) exhibited differences between both the free Qdots and the different conjugates of nQdot-origami. Origami having larger numbers of bound Qdots diffused more slowly. Unfortunately, the observed distributions of D for the nQdot-origami overlap, so

measurements of D alone are not sufficient to determine the identity of an individual tracked species.

We use the distributions of D values to estimate the hydrodynamic radii of free Qdots and each nQdot-origami conjugate using the Stokes-Einstein equation, $D = kT/(6\pi\eta R)$, wherein k is Boltzmann's constant, T is temperature, η is the viscosity of the medium, and R is the particle radius.[9] The value of η for the glycerol/buffer mixture employed used for these calculations was 10 x 10^{-3} Pa·s.[13] The hydrodynamic diameter of free Qdot is determined to be (26 ± 3) nm, in good agreement with previous work.[14] The hydrodynamic diameter (d_h) of nQdot-origami increases as n increases (Table 1).

Table 1. Measured diffusion coefficients of various nQdot-origami conjugates and their hydrodynamic diameters calculated from D. Errors in D are the standard deviations of the respective Gaussian fits.

	Free Qdot	1Qdot-Origami	2Qdots-Origami	3Qdots-Origami
D (μm^2·s^{-1})	1.69 ± 0.16	0.63 ± 0.07	0.49 ± 0.06	0.41 ± 0.05
d_h (nm)	26 ± 3	69 ± 7	88 ± 9	105 ± 10
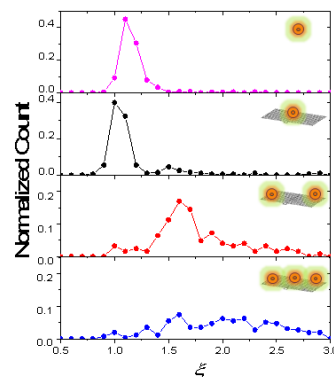
Fig. 4 Normalized ξ distribution of free Qdot and DNA origami with 1, 2 and 3 Qdots.

While measurements of D alone are not sufficient to unambiguously identify a tracked species, the combination of D with $g^2(\tau)$ values can provide a clear separation. $g^2(\tau)$ measures the correlation between the light field intensity with that after a delay, τ, and is used to identify single-photon sources.[10,11] An ideal single-photon source, is expected to have a $g^2(\tau = 0)$ of zero, since two photons cannot be emitted simultaneously. For multiple single-photon sources, $g^2(\tau = 0)$ will increase with the number of sources as simultaneous photon detection events become more probable. Measurement of $g^2(\tau)$ for the different fluorescent species in the reaction system therefore provides an additional means of quantifying the number of bound species (Fig. S4). We calculate the mean number of single-photon emitters (Qdots), ξ with $g^2(\tau = 0)$, using the equation, $\xi = 1/[1-g^2(\tau = 0)]$ to provide an estimate of the number of Qdots bound to an individual origami.[15] We note that ξ is a continuously varying parameter because of Qdot blinking and bleaching. For both free Qdot and 1Qdot-origami, the distributions of ξ are sharp and exhibit a maximum at $\xi = 1$, indicating that there is a single Qdot. Although the ξ distributions for 2Qdot-origami and 3Qdot-origami are broader (Full Width Half Maximum > 1) than those for free Qdots and 1Qdot conjugates, they can be clearly

distinguished from those for a single Qdot emitter. While the separation between the peaks of the 2Qdot and 3Qdot distributions is not marked, the peaks lie at values of ξ less than two and three, respectively, and the distributions are broad and overlap considerably. This reflects the fact that, during the photon collection time, not all of the bound Qdots are emitting constantly.
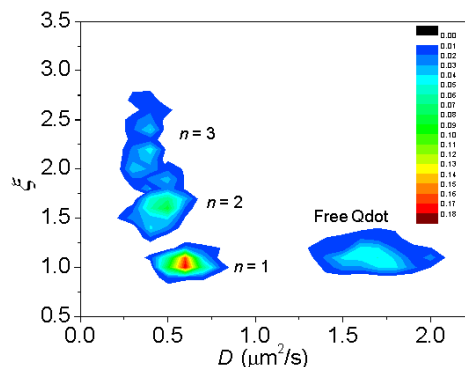
Fig. 5 Combined distribution plot of ξ and D of free Qdot and DNA origami with 1, 2 and 3 Qdots.

Although, singly, both the measured values of D and ξ produce overlapping distributions for the various nQdot-origami species, in combination clearly separable distributions for all four species present are obtained (Fig. 5).
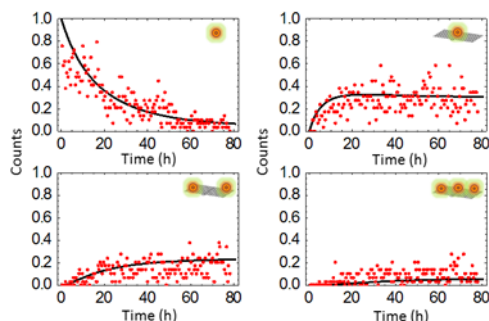
Fig. 6 Binding process of Qdots to DNA origami with three binding sites. Red dots represent the normalized observed counts (number observed in 30 min increments normalized to free Qdot count at the start of the experiment) of each species and the black solid line is a fit using Becker-Döring reaction rate equations[16] assuming the same attachment and detachment rate coefficients for all binding and unbinding steps. The rate coefficients determined from the fit are not physical due to the counting biases for the different species.

Having made an assignment for each tracked particle on the basis of the two-dimensional D-ξ distribution, we can now follow the evolution of the populations of the various reaction products over time (Fig. 6). The concentration of free Qdots falls rapidly as the reaction progresses, and is coincident with an increase, first in the number of 1Qdot-origami, then 2Qdot-origami, and then finally 3Qdot-origami. Although the number of Qdots is designed to be approximately the same as the total number of binding sites available, we do not expect to see the reaction go to completion, even with the high affinity between Qdots and binding sites because the concentrations of the reagents are in the picomolar range.

In summary, we have directly monitored the binding process of Qdots to DNA origami containing single and multiple binding sites using a single-particle tracking system. Diffusion coefficients and single-photon statistics of the reaction products were measured on an individual particle basis and, in combination, enable accurate identification of the tracked species to be performed with the samples in their native environment, without any isolation or purification. In the future quantitative data on reaction rates will be obtained by using the measured diffusion coefficients of each species, the capture volume of the tracking system, and the mean time between capture events to provide an estimate of the actual concentration of each species.

Notes and references

[a] Center for Nanoscale Science and Technology, National Institute of Standards and Technology, Gaithersburg, MD 20899, USA. Fax: 301-975-5314; Tel: 301-975-6050; E-mail: liddle@nist.gov, ajberglund@gmail.com
[b] Maryland Nanocenter, University of Maryland, College Park, MD 20742, USA.

1   P.W. K. Rothemund, *Nature,* 2006*,* **440**, 297.
2   J. Sharma, R. Chhabra, C. S. Andersen, K. V. Gothelf, H. Yan and Y. Liu, *J. Am. Chem. Soc.*, 2008, **130**, 7820.
3   L. A. Stearns, R. Chhabra, J. Sharma, Y. Liu, W. T. Petuskey, H. Yan and J. C. Chaput, *Angew. Chem. Int. Ed.*, 2009, **48**, 8494.
4   A. M. Hung, C. M. Micheel, L. D. Bozano, L. W. Osterbur, G. M. Wallraff and J. N. Cha, *Nature Nanotech.*, 2010, **5**, 121.
5   S. Pal, Z. Deng, B. Ding, H. Yan and Y. Liu, *Angew. Chem. Int. Ed.*, 2010, **49**, 2700.
6   B. Ding, Z. Deng, H. Yan, S. Cabrini, R. N. Zuckermannn and J. Bokor, *J. Am. Chem. Soc.*, 2010, **132**, 3248.
7   H. Bui, C. Onodera, C. Kidwell, Y. Tan, E. Grauangard, W. Kuang, J. Lee, W. B. Knowlton, B. Yurke and W. L. Hughes, *Nano Lett.*, 2010, **10**, 3367.
8   S. H. Ko, G. M. Gallatin and J. A. Liddle, *Adv. Funct. Mater.,* 2012, **22**, 1015.
9   K. McHale, A. J. Berglund and H. Mabuchi, *Nano Lett.,* 2007*,* **7**, 3535; K. Du, J. A. Liddle, A. J. Berglund *, Langmuir* 2012, **28**, 9181.
10   Second-order photon correlation function is defined as: $g^2(\tau) = \langle I(t)I(t+\tau)\rangle/\langle I(t)\rangle\langle I(t+\tau)\rangle$ where $I(t)$ is the fluorescence intensity at time t. $g^2(\tau)$ measures the joint probability of detecting the arrival of a photon at time t and another time $t+\tau$. When observing a single Qdot, the correlation function shows a dip at zero time delay: $g^2(\tau = 0) \approx 0$ (See Fig. S4).
11   V. Zwiller, H. Blom, P. Jonsson, N. Panev, S. Jeppesen, T. Tsegaye, E. Goobar, M.-E. Pistol, L. Samuelson and G. Björk, *Appl. Phy. Lett.,* 2001, **78**, 2476.
12   The standard deviation, S_D, of each measurement of D is $S_D = 0.3D$. A detailed discussion is given in the SI.
13   We used viscosity which was already known based on glycerol concentration and the value of viscosity was confirmed by measurements using polystyrene nanoparticles.
14   J. C. Rife, J. P. Long, J. Wilkinson, and L. J. Whitman, *Langmuir*, 2009, **25**, 3509.
15   P. Tinnefeld and M. Sauer, *Angew. Chem. Int. Ed.*, 2005, **44**, 2642.
16   T. Chou and M. R. D'Orsogna, *Phys. Rev. E*, 2011, **84**, 011608.